

# Spherical Harmonic Amplitudes From Grid Data

**Mark E. Rupright**

Florida Atlantic University  
The Harriet L. Wilkes Honors College  
5353 Parkside Dr. Jupiter, FL 33458

E-mail: [rupright@fau.edu](mailto:rupright@fau.edu)

**Abstract.** The problem of resolving spherical harmonic components from numerical data defined on a rectangular grid has many applications, particularly for the problem of gravitational radiation extraction. A novel method due to Misner improves on traditional techniques by avoiding the need to cover the sphere with a coordinate system appropriate to the grid geometry. This paper will discuss Misner's method and suggest how it can be improved by exploiting local regression techniques.

PACS numbers: 04.25.Dm, 02.30.Mv, 02.30.Px, 02.60.Ed

## 1. Introduction

Spherical harmonic decomposition is an important tool in computational science. In numerical astrophysics, for example, harmonic decomposition can serve as the basis of an algorithm for extracting gravitational waveforms from simulations of radiating systems. [1, 2, 3]

Harmonic decomposition of data defined on a two-sphere is a straightforward computation. Consider a scalar field  $\Phi(t, r_0, \theta, \phi)$  defined on a two-sphere of radius  $r_0$ . The field can be expanded in terms of scalar spherical harmonics as

$$\Phi(t, r_0, \theta, \phi) = \sum_{\ell, m} \Phi^{\ell m}(t, r_0) Y_{\ell m}(\theta, \phi) .$$

The orthonormality of the spherical harmonics with respect to integration over the sphere can be used to compute the harmonic amplitudes

$$\Phi^{\ell m}(t, r_0) = \oint \bar{Y}_{\ell m}(\theta, \phi) \Phi(t, r_0, \theta, \phi) d^2\Omega , \quad (1)$$

where the bar denotes complex conjugation.

Of interest for numerical analysis are cases in which the field  $\Phi$  is not known as an analytic function on the sphere, but rather as the solution of, for example, a wave equation evolved on a discrete set of points  $\{x_i\}$  which comprise a three-dimensional grid for the numerical simulation. In general these grid points will not lie on the sphere  $r = r_0$ . Therefore, computing the harmonic coefficients  $\Phi^{\ell m}$  from (1) requires a method of determining field values on the integration sphere.

The most obvious method of computing  $\Phi^{\ell m}$  from grid data is first to interpolate data from the grid onto coordinate patches covering the two-sphere, then compute a numerical integral of the interpolated data against the conjugate spherical harmonics. Because the grid data is the source of all information about  $\Phi$ , it is important that the coordinate patches on the two-sphere adequately represent the distribution of three-dimensional grid points near the sphere. For example, a spherical coordinate grid discretized in  $\{\theta, \phi\}$  will over-represent points near the poles and under-represent points near the equator.

Previous investigations of the the gravitational radiation extraction problem used a pair of stereographic coordinate patches to cover the sphere [1]. These patches, due to Gómez, *et al* [4], overlapped at the equator and special care was required to compute the integrals of (1) correctly. A useful alternative is to use ‘‘cubed sphere’’ coordinates like those used by Zink, *et al* [3]. In these coordinates the six patches represent cartesian grids, deformed to cover a sphere, which join nicely at the patch boundaries. The distribution of points in these patches is approximately uniform and close to the distribution of nearby grid points.

Misner has proposed an attractive alternative approach to the multipole decomposition problem that replaces the traditional two-step interpolation/integration method with a single volume integration step for each mode [5]. In addition to the computational simplification offered by this approach, Misner’s method completely

bypasses the need to choose a coordinate grid covering the two-sphere. Instead, it relies directly on values of  $\Phi$  on the grid points surrounding the sphere. The relative weight of each point in the calculation depends only on its proximity to the sphere.

Fiske [6] has recently presented an analysis of symmetry and convergence properties of Misner's method, and Fiske, *et al* [2] have demonstrated its usefulness in extracting gravitational radiation from cubical grids with fixed mesh refinement.

This paper presents an alternative analysis of Misner's algorithm which exploits the fact that it can be cast as a weighted local least-squares regression procedure. This approach somewhat simplifies the computational aspects of Misner's method, and improves the accuracy of the calculations.

While the analysis in this paper will assume complex-valued harmonics, test computations on a real-valued scalar field will be performed using real-valued spherical harmonics for simplicity. The test function will be the analytical quadrupole solution of a three-dimensional linear scalar wave equation. Specifically, the test function will be  $\Phi(t, r, \theta, \phi) = \Phi^{20}(t, r)Y_{20}(\theta, \phi)$ , where  $\Phi^{20}$  is constructed from a generating function of the form  $(x/\lambda^2)\exp(-x^2/\lambda^2)$ , and  $x = t \pm r$ . The initial data is time-symmetric and we choose unit wavelength ( $\lambda = 1$ ) and amplitude. This is similar to the wave evolved by Fiske, *et al* [2], but here  $\Phi$  is the solution of a linear, scalar wave equation. The computational grid extends from  $-8$  to  $8$  with uniform spacing  $h$  in each dimension. Multipole amplitudes are computed from this test data on a two-sphere of radius  $r_0 = 6$ . Most computations are performed in the first octant with even reflection symmetry imposed at the coordinate plane boundaries.

## 2. Misner's Algorithm

### 2.1. Continuum Limit

Recognizing that a surface integral like (1) can be treated as the derivative of a volume integral, Misner approaches the problem of computing harmonic coefficients by integrating data over a specified volume surrounding the two-sphere. The volume of interest is a spherical shell,  $S$ , of half-width  $\Delta$  that surrounds the sphere:

$$S = \{x \equiv \{r, \theta, \phi\} \mid r \in [r_0 - \Delta, r_0 + \Delta]\} .$$

He then expands the field  $\Phi$  not only in terms of orthonormal basis functions in  $\{\theta, \phi\}$  (spherical harmonics), but also in terms of radial basis functions  $R_n(r)$  ( $n = 0, \dots, \infty$ ) that are orthonormal with respect to integration over the radial interval  $[r_0 - \Delta, r_0 + \Delta]$ :

$$\int_{r_0 - \Delta}^{r_0 + \Delta} \bar{R}_n(r) R_m(r) r^2 dr = \delta_{nm} . \quad (2)$$

The tensor product of the radial and angular basis functions represents a new set of three-dimensional basis functions that are orthonormal with respect to integration over the shell  $S$ . These can be written as

$$Y_A \equiv Y_{n\ell m} = R_n(r) Y_{\ell m}(\theta, \phi) ,$$

where the single index  $A \equiv \{n \ell m\}$  denotes the three indices that identify the three-dimensional basis functions.

Specifically, Misner uses Legendre polynomials  $P_n$  to generate the (real-valued) radial basis functions

$$R_n(r) = \frac{1}{r} \sqrt{\frac{2n+1}{2\Delta}} P_n\left(\frac{r-r_0}{\Delta}\right),$$

which satisfy (2). The choice of Legendre polynomial as the basis for  $R_n$  is not unique and other choices will be investigated later.

The integral over  $S$  defines an inner product for functions defined on the shell:

$$\langle f|g \rangle \equiv \int_S \bar{f}(x) g(x) d^3x,$$

where the bar denotes complex conjugation. The orthonormality relation can be expressed as  $\langle Y_{A'}|Y_A \rangle = \delta_{A'A} \equiv \delta_{n'n} \delta_{\ell'\ell} \delta_{m'm}$ .

The expansion of  $\Phi$  in terms of these basis functions is

$$\Phi(t, x) = \sum_A \Phi^A(t) Y_A(r, \theta, \phi),$$

where the coefficients of the expansion are  $\Phi^A(t) = \langle Y_A|\Phi \rangle$ . The harmonic coefficients at  $r_0$  are expressed in terms of the coefficients  $\Phi^A$  as:

$$\Phi^{\ell m}(t, r_0) = \sum_n R_n(r_0) \Phi^{n\ell m}(t) = \sum_n R_n(r_0) \langle Y_{n\ell m}|\Phi \rangle. \quad (3)$$

It is useful to re-cast (3) in terms of a set of projection functions,

$$p^{\ell m}(x) = \left\{ \sum_n R_n(r_0) R_n(r) \right\} \bar{Y}_{\ell m}(x), \quad (4)$$

that act on  $\Phi$  under the inner product to give the harmonic amplitudes:

$$\Phi^{\ell m}(t, r_0) = \langle p^{\ell m}|\Phi \rangle = \int_S p^{\ell m}(x) \Phi(t, x) d^3x. \quad (5)$$

## 2.2. Numerical Approximation

Misner's algorithm is based on a specific method of converting the continuum integral above into a numerical integral over the grid points located within the shell  $S$ . By assuming a cell-centered grid of uniform spacing  $h$  (cell volume  $h^3$ ), one can approximate a volume integral by a sum that is equivalent to a "midpoint" quadrature:

$$\sum_{x_i \in S} \bar{f}(x_i) g(x_i) h^3 \approx \int_S \bar{f}(x) g(x) d^3x, \quad (6)$$

ignoring effects near the boundary of  $S$ .

Of course some points near the shell boundary belong to cells that do not lie entirely within  $S$ , while other points located just outside the boundary belong to cells that lie partially within the shell. To account for this effect, Misner adds to the sum (6) all points a distance less than  $\frac{1}{2}h$  *outside* of  $S$ . The correct inner product uses points from

a larger shell, which we shall denote  $S_+$ , defined to be the set of all grid points that lie within a radial distance  $\delta \equiv \Delta + \frac{1}{2}h$  of  $r_0$ . Furthermore, all points that lie “near” the shell boundary are weighted based on the partial volume of their cell that lies within  $S$ .

Keeping track of these partial volumes is complicated, but a simple approximation is to treat each point near the boundary as if it lay on a coordinate axis. This makes the partial volume a linear function of  $r$ :

$$w(r_i) = \begin{cases} 0 & |r_i - r_0| > \delta \\ h^3 & |r_i - r_0| < \delta - h \\ (\delta - |r_i - r_0|) h^2 & \text{otherwise,} \end{cases}$$

where  $r_i$  is the radial coordinate of point  $x_i$ . Other choices of weight function will be discussed below.

In Misner’s method, computations of the harmonic coefficients from grid data are based on the numerical inner product

$$\langle f|g \rangle \equiv \sum_{x_i \in S_+} \bar{f}(x_i) g(x_i) w(r_i). \quad (7)$$

In the continuum limit, the inner product of basis functions is equivalent to the identity matrix. However, because the weighted sum of (7) is only an approximation to the continuum integral, the basis functions  $Y_A$  are not strictly orthonormal and the numerical inner product defines a matrix  $G_{AB} = \langle Y_A|Y_B \rangle$  that approximates the identity. While some matrix elements of  $G_{AB}$  will be identically zero due to symmetries, the remaining elements will only approximate their continuum values to a degree determined by the numerical approximation. As a result, using the numerical inner product (7) in the calculation of (3) gives a convergent set of values of  $\Phi^{\ell m}(t, r_0)$ , but could result in mode mixing.

We can avoid this by using the inverse of the inner product matrix,  $G^{AB} \equiv (G_{AB})^{-1}$ , to define a set of *dual* basis functions  $Y^A = \sum_B G^{AB} Y_B$  that are orthonormal to the original basis with respect to the inner product:

$$\langle Y^A|Y_B \rangle = \sum_C G^{AC} \langle Y_C|Y_B \rangle = \sum_C G^{AC} G_{CB} = \delta_B^A.$$

Using the dual basis functions, define the expansion coefficients  $\Phi^A$  using the inner product with the dual basis

$$\Phi^A \equiv \langle Y^A|\Phi \rangle = \sum_B G^{AB} \langle Y_B|\Phi \rangle, \quad (8)$$

using the numerical inner product (7). This choice defines an approximation to the original data,  $\hat{\Phi} \equiv \sum_A \Phi^A Y_A \approx \Phi$ . For a given *finite* collection of basis functions, the approximation  $\hat{\Phi}$  minimizes the (weighted) sum of the squared differences between  $\Phi(x_i)$  and  $\hat{\Phi}(x_i)$  over the grid points in  $S_+$ . In other words, Misner has replaced the interpolation/spherical integration with a least squares procedure to compute spherical harmonic coefficients.

The projection functions of (4) can be computed at the beginning of a simulation from the dual basis functions  $Y^A$  and stored for future use. At each time step of a

simulation, the approximate spherical harmonic amplitudes  $\Phi^{\ell m}(t, r_0)$  are computed from the numerical inner product of the projection functions with the field  $\Phi$

$$\Phi^{\ell m}(t, r_0) = \langle p^{\ell m} | \Phi \rangle = \sum_{x_i \in S_+} p^{\ell m}(x_i) \Phi(t, x_i) w(r_i).$$

### 3. The Least-squares Perspective

In their analyses, Misner and Fiske focus mostly on the relation between the weighted sums and the underlying three-dimensional integrals they approximate. It is useful, however, to consider Misner's method strictly as a least-squares problem.

#### 3.1. Matrix Form

Focusing on the least-squares aspect of the method makes it easier to see how to compute the projection operators that will be used in the computation of the harmonic amplitudes. It is useful to re-cast the algorithm in the traditional matrix notation of linear regression analysis.

Let  $N$  be the number of points in the computational shell  $S_+$ , and  $M$  be the number of independent modes  $A \equiv \{n, \ell, m\}$  over which the three-dimensional harmonic expansion is performed. Let  $\Phi$  be the  $N \times 1$  column vector of values of  $\Phi$  at all points in  $S_+$ . Similarly, let  $\mathbf{Y}$  be the  $N \times M$  design matrix, where each column of  $\mathbf{Y}$  is one of the  $M$  basis functions  $Y_A$  evaluated at all points in the shell. Finally, let  $\mathbf{W}$  be the  $N \times N$  diagonal matrix of weights  $w_i$ . Then  $G_{AB}$  is easily computed as  $\mathbf{G} \equiv \mathbf{Y}^\dagger \mathbf{W} \mathbf{Y}$ , where  $\mathbf{Y}^\dagger$  is the Hermitian conjugate of  $\mathbf{Y}$ .

Denote the set of expansion coefficients  $\Phi^A$  as the  $(M \times 1)$  column vector  $\mathbf{F}$ . The vector of approximate values,  $\hat{\Phi} \approx \Phi$  in  $S_+$ , is  $\hat{\Phi} = \mathbf{Y} \mathbf{F}$ . The weighted sum of squared residuals (SSR) between  $\Phi$  and  $\hat{\Phi}$  is  $(\Phi - \mathbf{Y} \mathbf{F})^\dagger \mathbf{W} (\Phi - \mathbf{Y} \mathbf{F})$ , and the expansion coefficient vector that minimizes the SSR is the familiar matrix solution of the least squares problem,

$$\mathbf{F} = (\mathbf{Y}^\dagger \mathbf{W} \mathbf{Y})^{-1} \mathbf{Y}^\dagger \mathbf{W} \Phi = \mathbf{G}^{-1} \mathbf{Y}^\dagger \mathbf{W} \Phi. \quad (9)$$

This is obviously equivalent to (8) above.

Let  $\mathbf{P} \equiv \mathbf{G}^{-1} \mathbf{Y}^\dagger \mathbf{W}$  be the projection matrix that computes the expansion coefficients when multiplied by the grid data:  $\mathbf{F} = \mathbf{P} \Phi$ . As in (4), appropriate linear combinations of rows of  $\mathbf{P}$  define a set of row vectors  $\mathbf{p}^{\ell m}$  that, when multiplied by the grid data, give the spherical harmonic amplitudes  $\Phi^{\ell m}(t, r_0) = \mathbf{p}^{\ell m} \Phi$ . These projection vectors are computed at the beginning of a simulation and stored for later use in computing the time-dependent expansion coefficients as the simulation evolves.

Of course it is not generally advisable to compute  $\mathbf{P}$  by inverting  $\mathbf{G}$ . It is better to compute the  $M \times N$  matrix  $\mathbf{P}$  as the solution of the linear system

$$\mathbf{G} \mathbf{P} = \mathbf{Y}^\dagger \mathbf{W}.$$

Because  $\mathbf{G}$  is a real, symmetric, positive-definite matrix, this system can be solved rapidly using Cholesky decomposition.

### 3.2. Weighting and Local Regression

There are actually two types of least-squares regressions involved in the method: a global regression of all points over the spherical harmonic basis functions, and a *local* regression over the radial basis functions. Local regressions differ from traditional global regression fits in that they are only used to compute the best-fit function at a specific point. In this case the local regression computes the spherical harmonic amplitudes at  $r = r_0$  from a fit over the interval  $(r_0 - \delta, r_0 + \delta)$ .

Local regression techniques are popular for data smoothing algorithms [7]. In such cases the value of a data point is replaced by the result of a weighted polynomial fit to it and neighboring points. A common, though not universal, feature of local regression techniques is that the weight of each point in the fit decreases with distance from the evaluation point. Two popular choices of local weight function are the “bisquare” function,

$$B(u) = \begin{cases} (1 - u^2)^2 & |u| < 1 \\ 0 & |u| \geq 1 \end{cases},$$

and the “tricube” function,

$$T(u) = \begin{cases} (1 - |u|^3)^3 & |u| < 1 \\ 0 & |u| \geq 1 \end{cases},$$

where  $u = (r - r_0)/\delta$  is a dimensionless radial coordinate defined so that the domain  $(r_0 - \delta, r_0 + \delta)$  is transformed to the interval  $(-1, 1)$ .

Contrast this with Misner’s method. In the continuum limit, all points weigh equally in the computation of  $\mathbf{G}$  because the Legendre polynomials are orthonormal with respect to integration over a constant weight function.

Now consider Misner’s weight in the numerical approximation, written in terms of the dimensionless radial coordinate  $u$ . Up to a multiplicative factor of  $h^3$  the weight function is

$$w(u) = \begin{cases} 0 & |u| > 1 \\ 1 & |u| < 1 - h/\delta \\ (1 - |u|) \delta/h & \text{otherwise.} \end{cases}$$

While the weight is constant for points near  $r_0$ , it falls off linearly for points near the edges of the shell  $S_+$ . The degree of down-weighting depends on the ratio of the size of the shell to the grid spacing,  $\delta/h$ . For  $\delta \gg h$ , the weights are essentially constant.

Figure 1 shows Misner’s weight function for two different values of  $\delta/h$  and compared to the bisquare and tricube weights. In his analysis of Misner’s method [6], Fiske finds that  $\delta = \frac{5}{4}h$  (equivalently,  $\Delta = \frac{3}{4}h$ ) gives good results in tests. In this case most points in  $S_+$  are “near” the boundary, and the weight function is local in the sense that it only emphasizes points nearest the center. In fact, Fiske’s choice leads to a weight function that is very similar in profile to the traditional local regression weights, and gives similar results.

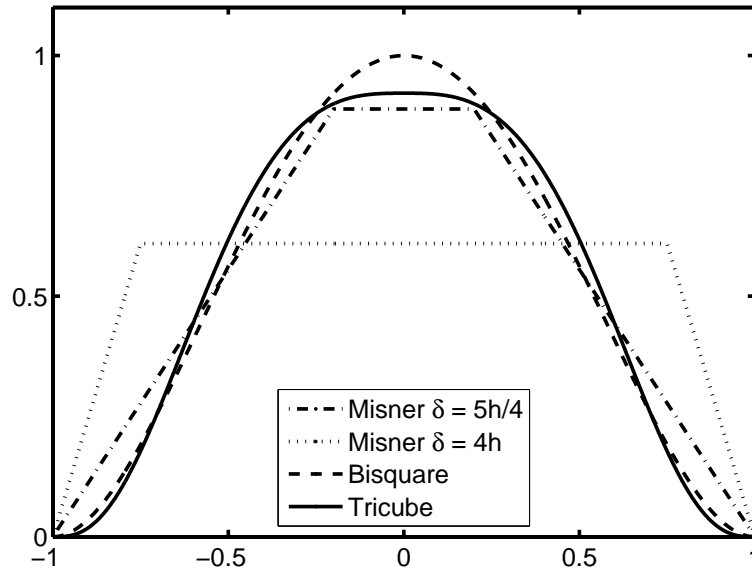


**Figure 1.** Comparison of Misner’s weights and local weights. The functions are scaled to have the same area underneath each curve.

To see the benefit of using local weights, consider Fiske’s analysis in the continuum limit. Misner’s method works because a linear combination of the radial basis functions  $R_n$  form a Dirac delta function:

$$\sum_{n=0}^{\infty} R_n(r_0) R_n(r) = r^{-2} \delta(r_0 - r) .$$

Given the definition of  $R_n$  in terms of the Legendre polynomials, define

$$d_P(u, N) \equiv \sum_{n=0}^N \left( \frac{2n+1}{2} \right) P_n(0) P_n(u) .$$

Note that only even values of  $n$  figure into this sum because  $P_n(0) = 0$  for odd  $n$ . The function  $d_P(u, N)$  will approach the Dirac delta function  $\delta(u)$  in the limit as  $N \rightarrow \infty$ . The use of a finite number of radial basis functions produces a truncation error that will have leading term  $O(\delta^{N+2})$ , so that a fit with  $N = 2$  or  $3$  will converge with shell size as  $O(\delta^4)$ .

The same analysis can be applied using functions that are orthonormal with respect to integration over the bisquare or tricube weight functions. Such orthogonal polynomials can be constructed using a Gram-Schmidt procedure. At least in the case of bisquare-weight functions, they can also be found by the simple Rodrigues formula

$$b_n(u) = c_n (1 - u^2)^{-2} \frac{d^n}{du^n} (1 - u^2)^{n+2} ,$$

where  $c_n$  is a normalization constant.



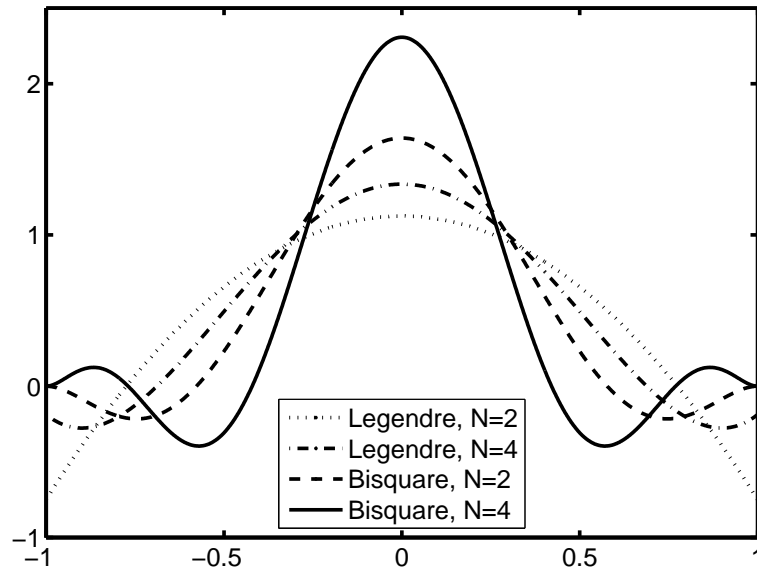


**Figure 2.** Comparison of  $d(u, N)$  constructed from Legendre and bisquare-weight polynomials.

The first few normalized bisquare-weight polynomials are

$$\begin{aligned} b_0(u) &= \sqrt{\frac{15}{16}} & b_1(u) &= \sqrt{\frac{105}{16}} u \\ b_2(u) &= \sqrt{\frac{45}{64}} (1 - 7u^2) & b_3(u) &= \sqrt{\frac{1155}{64}} (u - 3u^3) \\ b_4(u) &= \sqrt{\frac{1365}{2048}} (1 - 18u^2 + 33u^4) . \end{aligned}$$

Define

$$d_b(u, N) \equiv \sum_{n=0}^N b_n(0) b_n(u) (1 - u^2)^2 .$$

Again, this will approach  $\delta(u)$  in the limit  $N \rightarrow \infty$  and the leading order of truncation error is still  $O(\delta^{N+2})$ .

Figure 2 compares  $d_P$  and  $d_b$  for low orders. It is clear from the figure that the bisquare approximation to  $\delta(u)$  is better at each order than the Legendre approximation. This is because of the down-weighting inherent in local regressions.

The advantage of the local weighting is apparent in numerical tests. Figure 3 compares results of computations of  $\Phi^{20}$  from the test function using Misner's weight to those using the tricube weight. (Errors using the bisquare weight are close to, but slightly larger than, those using the tricube weight.) The vertical axis is the (base-10) log of the  $L_2$  norm of the error, while the horizontal axis is the log of  $\delta/h$ . The tests were performed using a quadratic fit in  $r$  ( $N = 2$ ).

The error in both plots in figure 3 is fourth-order convergent with respect to  $\delta$  (for fixed  $h$ ), as predicted by Fiske's analysis. The error using Misner's weight actually converges slightly faster than fourth-order because the shape of Misner's weight function changes with  $\delta/h$ , while the shape of the tricube weight is fixed. As  $\delta$  decreases, Misner's

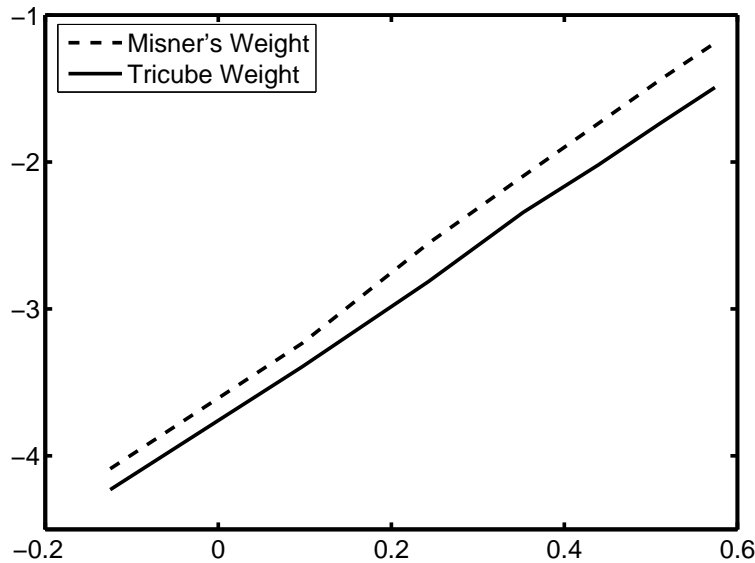


**Figure 3.** Comparison of  $\log(\text{error})$  to  $\log(\delta/h)$  for  $h = 1/8$ . The tricube error is 4th-order convergent, and the error for Misner's weight converges slightly faster.

weight function becomes more local, and it should be no surprise that Fiske found good results with  $\delta = \frac{5}{4}h$ . Regardless of the value of  $\delta/h$ , however, the bisquare and tricube weights will give better results than Misner's weight.

### 3.3. Switching to the monomial basis

The preceding analysis using Legendre and bisquare-weight polynomials is strictly correct in the continuum limit, not for calculations from grid data. In fact, the properties of Legendre polynomials in the continuum limit cannot be expected to carry over into the numerical regime, especially for small values of  $\delta$ , because the weight function will no longer be constant. Furthermore, because Misner's down-weighting prescription for boundary points is only correct for points near the coordinate axes, the orthonormality properties of the Legendre polynomials will break down in the numerical approximation for small shell sizes.

Of course this is not an problem in practice because Misner's method doesn't really rely on the computation of integrals. Instead, it is based on solving a weighted least squares problem and the only requirement for the radial basis functions is that they be linearly independent. It is quite simple (and useful in practice) to switch from an orthogonal polynomial basis to a monomial basis:

$$R_n(r) = \left( \frac{r - r_0}{\delta} \right)^n = u^n. \quad (10)$$

This choice simplifies the calculation by removing the need to form a linear combination of rows of  $\mathbf{P}$  to get the projection vectors  $\mathbf{p}^{\ell m}$ . On the contrary, because  $R_0(r_0) = 1$  and  $R_n(r_0) = 0$  for  $n > 1$ , then  $\Phi^{\ell m} = \Phi^{0 \ell m}$  and the rows of  $\mathbf{P}$  corresponding to  $n = 0$

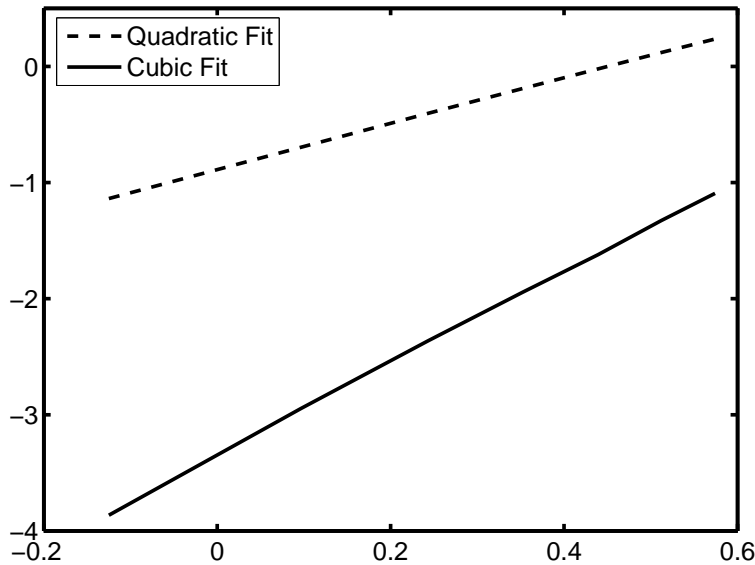


**Figure 4.** Comparison of errors in computation of  $d\Phi^{20}/dr$  for quadratic and cubic fits. The plot shows  $\log(\text{error})$  vs.  $\log(\delta/h)$  for  $h = 1/8$ .

for each  $\{\ell, m\}$  are the projection vectors  $\mathbf{p}^{\ell m}$ .

At this point, one may be concerned that the use of monomial basis functions might cause  $\mathbf{G}$  to become ill-conditioned. However, as long as the number of radial basis functions is small, this will not be a significant problem. Tests have shown that the difference between using the monomial basis and the orthogonal polynomial basis for a quadratic fit in  $r$  is on the order of the roundoff error expected from solving a linear system of that size.

An additional benefit of this approach comes in cases where the radial derivative of  $\Phi^{\ell m}$  is required at  $r_0$ . This is the case, for example, when the extracted multipole amplitudes at  $r_0$  are to be used as inner boundary data for the evolution of a one-dimensional second-order wave equation for each mode as in [1]. Based on the definition of  $R_n$  in (10), it is clear that the coefficient  $\Phi^{1\ell m}$  is the derivative (with respect to  $u$ ) of  $\Phi^{\ell m}$ . Therefore, we have  $(d\Phi^{\ell m}/dr)_{r=r_0} = \Phi^{1\ell m}/\delta$ . Again, this is easily computed using projection vectors that are rows of  $\mathbf{P}$ .

Fiske's analysis of truncation error in the approximation to the Dirac delta function also applies when computing  $d\Phi^{\ell m}/dr$ , only now it involves odd powers to approximate the derivative of the delta function. Here the error will converge as  $O(\delta^2)$  for a linear or quadratic fit, and will be  $O(\delta^4)$  for a cubic fit. Increasing the radial basis to include  $R_3$  will reduce the error in  $\Phi^{\ell m}$  by only a very small amount and will not improve the convergence properties of that error. However using a cubic fit to compute  $d\Phi^{\ell m}/dr$  offers significant improvement in both the error and its convergence properties, as shown in figure 4. Here we have a convenient rule of thumb: a quadratic fit in  $r$  is more than sufficient to compute the multipole amplitudes of  $\Phi$ , but a cubic fit is strongly suggested with the derivatives of those amplitudes are also required.

### 3.4. Symmetry issues

One final advantage of the least-squares perspective comes in its application to symmetry issues. Fiske [6] has studied extensively the symmetries of the basis functions  $Y_A$  and shown that the dual basis functions,  $Y^A$ , have the same symmetries. This is useful in cases where the three-dimensional simulation is computed in a single octant with explicit reflection symmetries at the coordinate planes. Fiske’s analysis shows how to apply Misner’s method in such cases by exploiting the symmetries of  $Y_A$  to compute the sums used to construct  $G_{AB}$ , which must be taken over all octants, using only data defined within the computational octant. The result is a block diagonal linear system constructed so that coefficients of harmonics that do not share the octant symmetry are forced to vanish.

Again, the least squares perspective offers a slightly different approach to the problem. First, because the least squares fit only relies on the basis functions being linearly independent, it is possible simply to perform the fit over all spherical harmonics using data in the octant. A problem with this approach is that it could cause  $\mathbf{G}$  to become ill-conditioned as the number of basis functions grows large.

A simple fix is to restrict the least squares fit to only those basis functions that share the octant symmetry of the simulation, and ignore all other basis harmonics. For example, because the test function in this paper is based on  $Y_{20}$ , the function  $\Phi$  will be even under reflection across the coordinate plane boundaries of the first octant. Using real-valued spherical harmonics, which are proportional to  $\cos(m\phi)$  for positive  $m$  and  $\sin(m\phi)$  for negative  $m$ , it is easy to show that the only harmonic functions that have this octant symmetry are those with even  $\ell$  and even, positive  $m$ . This guarantees that the fit matrix  $\mathbf{G}$  and the corresponding linear system are much smaller than those which use all spherical basis functions. A fit with  $\ell_{\max} = 2$ , could potentially involve nine angular basis functions, but only three of these ( $Y_{00}$ ,  $Y_{20}$ , and  $Y_{22}$ ) share the octant symmetry of  $Y_{20}$ . This cuts the size of linear system by a factor of three, significantly reducing computation time. While  $\mathbf{G}$  would no longer as sparse as in Fiske’s approach, this should not present a significant additional computational burden.

## 4. Discussion

Misner’s approach to the multipole decomposition of grid data offers a significant computational advantage over the traditional method of first interpolating grid data onto the two-sphere, then integrating against the spherical harmonics. For a shell size  $\delta$  that is proportional to the grid spacing  $h$ , fourth-order convergence is achieved by a simple least-squares fit over a quadratic polynomial in  $r$  and the specified set of basis functions (spherical harmonics) in  $\{\theta, \phi\}$ . This accuracy is achieved without the need to consider coordinate patches that cover the two-sphere.

The construction of projection vectors that can be computed at the beginning of a simulation and stored for use at each computational time level offers a significant

increase in computational speed, as well. While such operators can in principle be computed for the interpolation/integration method, their construction is significantly easier in Misner's method because the projection operators are simply the result of solving the linear system associated with a least squares regression problem.

Re-casting Misner's method as a local least squares problem does offer additional advantages in accuracy and computational simplicity. Tests suggest that a ( $r$ -dependent) tricube weighting scheme gives good results.

This analysis has not investigated the application of Misner's method to more complex problems that would use, for example, tensor harmonics. However, because the method is based only on the orthonormality of the basis functions (indeed, on the weaker requirement of linear independence) on the two-sphere, it should extend without difficulty to those problems.

We have also not investigated the application of Misner's method to mesh refinement. The analysis of Fiske, *et al* [2] demonstrates the simplicity of Misner's method to cases of *fixed* mesh refinement. Although it is not clear from that paper, a strict application of Misner's weighting scheme is slightly more complicated for refined grids than for the fixed grids considered here. This is because one must account for the fact that points in a refined region belong to cells with smaller volume  $h^3$ . However, from the local least-squares perspective the weight of each point only depends on its proximity to  $r_0$ . It is not clear that any advantage is gained by adjusting the weight of a point based on the density of grid points nearby.

Application to *adaptive* mesh refinement can complicate the process because there is no way *a priori* to establish the distribution of grid points at any given time level. This would seem to rule out pre-computing the projection vectors and slow down the procedure. However, because the computation is done over a shell that scales quadratically with resolution, this may not represent a significant time penalty.

More importantly, it may not even be necessary to consider adaptive mesh refinement when applying Misner's method. As long as the grid size, number of basis functions, and grid resolution are sufficient to compute the multipole amplitudes at the most coarse level, the multipole decomposition can be applied only to grid points on that level, and these are known *a priori*. Unless high-frequency modes are of interest, the values of the wave on the coarse grid should be sufficient to compute the multipole amplitudes.

## Acknowledgments

This research was funded by the FAU Division of Sponsored Research New Project Development grant #05-375.

## References

- [1] Rupright M E, Abrahams A M and Rezzolla L (1998) *Phys. Rev. D* **58** 044005

- [2] Fiske D R, Baker J G, van Meter J R, Choi D and Centrella J M 2005 *Phys. Rev. D* **71** 104036
- [3] Zink B, Pazos E, Diener P and Tiglio M 2006 *Phys. Rev. D* **73** 084011
- [4] Gómez R, Lehner L, Papadopoulos P and Winicour J 1997 *Class. Quantum Grav.* **14** 977–990
- [5] Misner C W 2004 *Class. Quantum Grav.* **21** S243–8
- [6] Fisk D R 2005 Error and Symmetry Analysis of Misner’s Algorithm For Spherical Harmonic Decomposition on a Cubic Grid *Preprint* gr-qc/0412047
- [7] Cleveland W S and Devlin S J 1988 *J. Amer. Statist. Assoc.* **83** 596–610